An Integrated Hidden Markov Model-Van der Pol Oscillator Based Atrial Fibrillation ECG Generator Model

Ayan Mukherjee
TCS Research
Tata Consultancy Services
Kolkata, India
ayan.m4@tcs.com

Oishee Mazumder
TCS Research
Tata Consultancy Services
Kolkata, India
oishee.mazumder@tcs.com

Aniruddha Sinha
TCS Research
Tata Consultancy Services
Kolkata, India
aniruddha.s@tcs.com

***Abstract*—In recent years stricter regulation of data privacy and protection has accelerated research in synthetic ECG time-series generation. With the increasing prevalence of Atrial Fibrillation (AF), its mathematical modelling remains an open research problem due to its unique and complex interval and morphological characteristics. The present research work presents an R-peak to R-peak (RR) interval distribution-aware integrated Hidden Markov Model-Van der Pol (HMM-VdP) oscillator based AF electrocardiogram (ECG) generator model. The approach consists of two parts: A HMM that is trained on RR intervals obtained from real-world AF ECG signals. The output of the trained HMM model is utilized to drive a coupled VdP oscillator model that is modified to generate synthetic ECG time-series with AF-like morphology. A final post-processing algorithm is applied on the output of the HMM-VdP oscillator model to get the synthetic AF time-series. The generated synthetic AF time series is evaluated comparatively with existing state-of-the-art dynamic AF models through qualitative (time-series morphology and Poincaré plot analysis) and quantitative (proposed metric) measures. The proposed AF model has shown significant improvement over the existing dynamic models. The proposed AF model can be utilized for AF detector evaluation, clinical training purpose.**

***Index Terms*—Atrial Fibrillation, ECG modelling, ECG synthesis, Hidden Markov Model, Van der Pol oscillator.**

I. Introduction

More than 32% of all global deaths are caused by cardiovascular diseases (CVDs) [1]. Physicians and clinicians rely on Electrocardiogram (ECG) as the primary diagnostic tool for the prognosis of CVDs and cardiac health monitoring. Availability of large real-world ECG datasets has ushered in a disruptive era of AI based solutions for cardiac monitoring and CVD detection in this current decade [2], [3]. However, two common limitations of such datasets are – I) skewed distribution of classes based on prevalence and II) enforcement of stricter regulations regarding data-privacy and data-sharing through laws like HIPPA [4] and nFADP [5]. Development of ECG models for generation of synthetic ECG data can potentially circumvent such limitations. Consequently, enhanced research efforts towards development of ECG models have been reported in recent years. [2] provides an expansive review of the existing sate-of-the-art (SoA) ECG modelling and synthetic ECG generation algorithms. Such modelling approaches can be broadly categorized under two classes: 1) mathematical models (MM) [6], [7], and 2) deep generative models [8], [9]. The MM category can be further sub-categorized into physiological, dynamic, and morphological models. While the physiological models aim to capture cardiac conduction at the cellular level, the morphological models target a single heart beat [2]. The purview of the present research work is the third subcategory: the dynamic models. The dynamic models aim to identify a set of mathematical equations that can mimic the typical ECG morphology (P, QRS, and T waves). [10] and [11], [12] are two seminal works in the dynamic ECG modelling domain. In [10], a dynamic model mimicking the cardiac conduction system is reported where the pace-makers are represented by modified Van der Pol-type (VdP) oscillators connected through time-delay velocity coupling and the heart muscle depolarization and repolarization processes are represented by modified FitzHugh–Nagumo model [13], [14]. The fact that not only normal sinus rhythm, but other pathological conditions like tachycardia and bradycardia are successfully modelled using this approach affirms its suitability for such purposes. Further modification of the model are reported to extend its capability to mimic pathological conditions like left and right bundle branch blocks [12].

Atrial fibrillation (AF) is a high-risk, high-prevalence arrhythmia characterized by irregular heart rhythm and rapid heart-rate [15]. The AF ECG morphology is markedly different from the quasi-periodic nature of the normal sinus rhythm [16] and thus its mathematical modelling offers unique research challenges. Mathematical model of AF can potentially aid in deeper understanding of the mechanism of AF, generating new insights [17]. While a few mathematical models of AF have been reported in recent years [18], [19], reliable mathematical modelling of AF through VdP-type oscillators remains an open research problem. The current research work proposes a novel hidden Markov model driven RR interval distribution-aware coupled Van der Pol oscillator based AF model.

The key research contributions of the work are as follows:

- A novel approach of modelling the AF specific RR intervals through hidden Markov model is proposed.
- A modified coupled Van der Pol type oscillator is proposed that incorporates the characteristic features of AF like the absence of P-waves and presence of fibrillatory f-waves.
- A novel HMM driven RR-interval distribution-aware coupled Van der Pol oscillator based AF model is proposed through integration of the above two approaches.
- The performance validation of the proposed AF model is done through qualitative and quantitative comparison with real-world AF data and existing state-of-the-art dynamic AF models.

The rest of the paper is structured as follows. Section II presents the details of the proposed AF model development methodology. Section III presents the validation result and comparative analysis of the proposed AF model's performance. Section IV prsents the concluding remarks.

II. Proposed Methodology

A. RR and δRR intervals of AF

While the typical RR-interval pattern gives AF its unique morphological characteristic, features derived from δRR are reported to be able to distinctively identify AF sequences [20]. This underscores the importance of δRR in characterizing AF sequences, and makes its consideration imperative for reliable MM of AF sequences. The statistical modelling approach of HMM, that develops probabilistic state transition models, learning from observable and underlying data, makes an appropriate choice for the present use-case of AF RR-interval modelling. For the training of the HMM, the instantaneous heart-rates are taken as the observations, and the δRRs are taken as the hidden states.

B. Hidden Markov Model: brief theoretical background

Hidden Markov model is a statistical tool that has been widely employed for the modelling of random processes in diverse fields like speech, bioinformatics, signal processing, etc [21]. It is based on the basic Markov chain assumption given in (1)

$$P(q_i = a|q_1.....q_{i-1}) = P(q_i = a|q_{i-1}) \tag{1}$$

for a sequence of state variables $q_1, q_2, ..., q_i$. A typical HMM model is defined by HMM(Q,A,B,π) where Q and A represents the set of states and transition probabilities respectively, B represents the observation likelihood/emission probabilities that expresses the probability of an observation o_t (drawn from a vocabulary $V = v_1, v_2, \cdots, v_v$) being generated from a state q_1 and π represents the initial probability distribution. The tutorial by Rabiner [22] provides a detailed description of the HMM algorithms and applications.

C. Integrated HMM-VdP based AF ECG model

The block diagram of the proposed integrated HMM-VdP based AF ECG model is shown in Fig. 1. The VdP part of the proposed integrated model is based on the modification

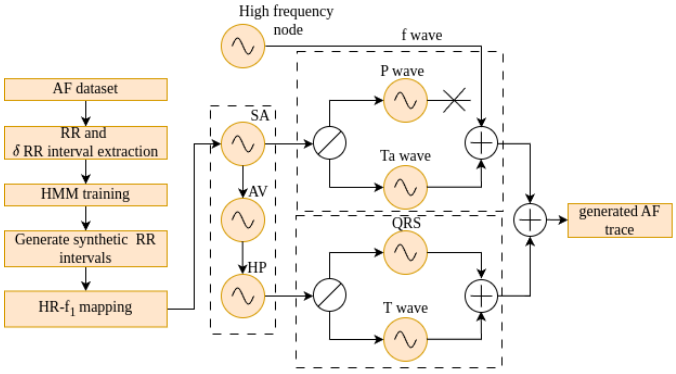

Fig. 1. Block diagram of the integrated HMM-VdP based AF ECG model

of the VdP model reported in [12] for bundle block disease modelling. For the model, four oscillators are used to represent the sino-atrial (SA), atrio-ventricular (AV) nodes, and the right and the left bundle branches (RB, LB) of the His-Purkinje (HP) system. Further, the FitzHugo–Nagumo equations are utilized to model the electrical process in the cardiac muscles. (2) to (5) represents the dynamics of the natural pacemakers and the HP fibres, where $x_i(t)$ and $y_i(t)$ represent the action potential and the transmenbrane currents of the heart, $a_i(x_i - u_{ik})$ are the damping factors, $f_i x_i(x_i - d_{ij})(x_i - e_{ik})$ are the harmonic force terms, $a_i > 0$, u_{ij} represent the non-linear damping force parameters, f_i are the parameters related to the intrinsic frequency of the oscillator, the coupling coefficients k_{SA-AV} and k_{AV-HP} represent the unidirectional coupling between the pacemakers SA, AV and HP.

Further, the depolarization and the repolarization of the atrial and ventricular muscles are represented by Fitzhugh-Nagumo model as given in (6) to (9). Finally the activation currents I_i that represents the coupling between the SA and the atrial muscles and between the RB-LB pacemakers and the ventricular muscles are represented by (10) to (13). The values of the parameters except f_1 are identical to those reported in [12].

$$SA = \begin{cases} \dot{x}_1 = y_1, \\ \dot{y}_1 = -a_1 y_1(x_1 - u_{11})(x_1 - u_{12}) \\ \qquad - f_1 x_1(x_1 + d_1)(x_1 + e_1) \end{cases} \tag{2}$$

$$AV = \begin{cases} \dot{x}_2 = y_2, \\ \dot{y}_2 = -a_2 y_2(x_2 - u_{21})(x_2 - u_{22}) - f_2 x_2 \\ (x_2 + d_2)(x_2 + e_2) + K_{SA-AV}(x_1 - x_2) \end{cases} \tag{3}$$

$$RB = \begin{cases} \dot{x}_{3_{RB}} = y_{3_{RB}}, \\ \dot{y}_{3_{RB}} = -a_3 y_{3_{RB}}(x_{3_{RB}} - u_{31})(x_{3_{RB}} - u_{32}) - f_3 x_{3_{RB}} \\ \qquad (x_{3_{RB}} + d_3)(x_{3_{RB}} + e_3) + K_{AV-RB}(x_2 - x_{3_{RB}}) \end{cases} \tag{4}$$

$$LB = \begin{cases} \dot{x}_{3_{LB}} = y_{3_{LB}}, \\ \dot{y}_{3_{LB}} = -a_3 y_{3_{LB}}(x_{3_{LB}} - u_{31})(x_{3_{LB}} - u_{32}) - f_3 x_{3_{LB}} \\ \qquad (x_{3_{LB}} + d_3)(x_{3_{LB}} + e_3) + K_{AV-LB}(x_2 - x_{3_{LB}}) \end{cases} \tag{5}$$

$$Pwave = \begin{cases} \dot{z_1} = k_1(-c_1 z_1(z_1 - w_{11}(z_1 - w_{12}) - b_1 v_1 \\ \qquad\qquad - d_1 v_1 z_1 + I_{AT_{De}}), \\ \dot{v_1} = k_1 h_1(z_1 - g_1 v_1) \end{cases} \tag{6}$$

$$T_a wave = \begin{cases} \dot{z_2} = k_2(-c_2 z_2(z_2 - w_{21}(z_2 - w_{22}) - b_2 v_2 \\ \qquad\qquad - d_2 v_2 z_2 + I_{AT_{Re}}), \\ \dot{v_2} = k_2 h_2(z_2 - g_2 v_2) \end{cases} \tag{7}$$

$$QRS = \begin{cases} \dot{z_3} = k_3(-c_3 z_3(z_3 - w_{31}(z_3 - w_{32}) - b_3 v_3 \\ \qquad\qquad - d_3 v_3 z_3 + I_{VN_{De}}), \\ \dot{v_3} = k_3 h_3(z_3 - g_3 v_3) \end{cases} \tag{8}$$

$$Twave = \begin{cases} \dot{z_4} = k_4(-c_4 z_4(z_4 - w_{41}(z_4 - w_{42}) - b_4 v_4 \\ \qquad\qquad - d_4 v_4 z_4 + I_{VN_{Re}}), \\ \dot{v_4} = k_4 h_4(z_4 - g_4 v_4) \end{cases} \tag{9}$$

$$I_{AT_{De}} = \begin{cases} 0, & \text{for } y_1 \leq 0, \\ K_{AT_{De}} y_1 & \text{for } y_1 > 0, \end{cases} \tag{10}$$

$$I_{AT_{Re}} = \begin{cases} -K_{AT_{Re}} y_1, & \text{for } y_1 \leq 0, \\ 0 & \text{for } y_1 > 0, \end{cases} \tag{11}$$

$$I_{VN_{De}} = \begin{cases} 0, & \text{for } y_{3_{HP}} \leq 0, \\ K_{VN_{De}}(y^{tot}_{3_{RB}} + y^{tot}_{3_{LB}}) & \text{for } y_{3_{HP}} > 0, \end{cases} \tag{12}$$

$$I_{VN_{Re}} = \begin{cases} -K_{VN_{Re}}(y^{tot}_{3_{RB}} + y^{tot}_{3_{LB}}), & \text{for } y_{3_{HP}} \leq 0, \\ 0 & \text{for } y_{3_{HP}} > 0, \end{cases} \tag{13}$$

f_1 is a key parameter of the VdP system that controls the intrinsic oscillation of the AV node. The non-linear relationship that exists between f_1 and the AV oscillation rate is shown in Fig. 2. Leveraging this relationship, a modification in the existing VdP model is introduced in the form of an additional oscillator node with high f_1 values scaled by a random multiplier to model the fibrillatory f-waves. Additionally, the output of (6) is disconnected from the output to realize the absence of P-wave. The trained HMM model is integrated with the modified coupled VdP system through an interface that maps each element of the synthetic HR vector (generated by the trained HMM model) to its corresponding f_1 value. The f_1 value then controls the VdP system to generate ECG sequence with target RR-interval.

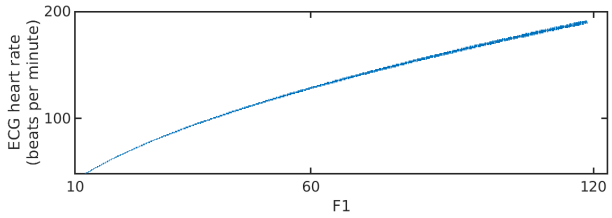

Fig. 2. Mapping between f_1 and ECG heart rate

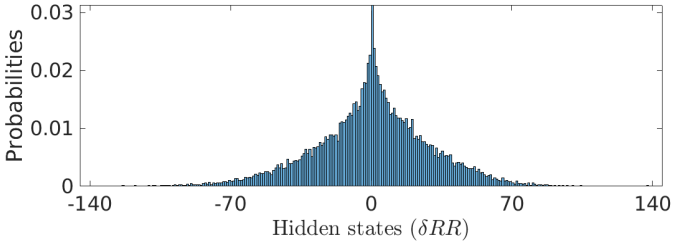

Fig. 3. Histogram of the states

III. Result and Discussion

A. Training of the proposed AF model

The proposed integrated HMM-VdP oscillator based AF model is realized in the MATLAB-Simulink computational environment. A subset of the publicly available PhysioNet Challenge 2017 [23] training dataset, containing 758 AF annotated ECG recordings, henceforth referred to as PNC17AFDB, is used for training and validation of the proposed model. For the purpose, the PNC17AFDB is split into training and testing subsets in the ratio of $80 : 20$. For the training purpose, the R-peak indices of the PNC17AFDB are extracted using the modified Pan-Tompkin's algorithm [24]. Now, the HMM model is trained with the derived RR and δRR sequences taken as the emissions and the hidden states respectively. For this training purpose, the iterative Forward-Backward algorithm is utilized. The distribution of the hidden states are shown in Fig. 3. The count of the hidden sates is reduced to 73 through quantization. The state-emission probability matrix as learnt by the HMM model is plotted in Fig. 4. The probabilities are plotted in the logarithm scale for prominence. The trained HMM model is then utilized to generate 200 vectors of HR sequences, each containing 120 elements. The distribution of

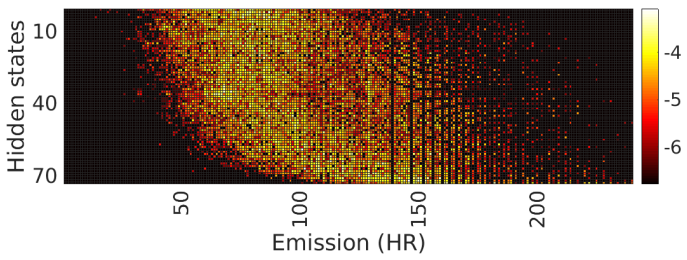

Fig. 4. Plot of emission probabilities

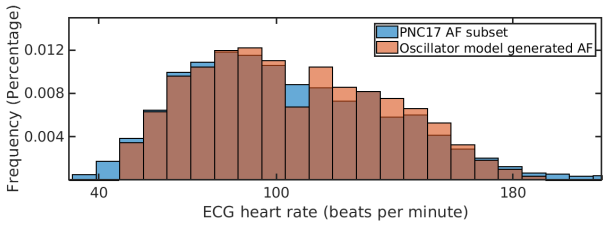

Fig. 5. Comparison of synthetic and real-world AF heart-rate distribution

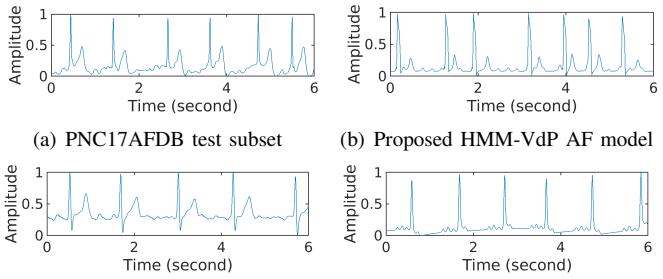

(a) PNC17AFDB test subset (b) Proposed HMM-VdP AF model

(c) SoA1 paroxysmal AF model (d) SoA2 Gaussian wave AF model

Fig. 6. Sample plots of real-world AF time-series and synthetic AF time-series generated by the proposed HMM-VdP AF model and existing SoAs

the generated synthetic HRs and the corresponding distribution of the PNC17AFDB test subset are plotted in Fig. 5. The significant overlap between the two distributions validates the efficacy of the HMM model in capturing the typical AF heart rate (HR) characteristics.

Finally, the generated HR vectors are utilized to generate the ECG sequences from the modified VdP oscillator system as discussed in the preceeding section, through modulation of the f_1 parameter.

B. Performance evaluation of the proposed AF model

The evaluation framework for the performance analysis of the proposed AF model is designed considering the two clinically relevant characteristic features of AF - irregularly regular RR intervals and absence of the P waves. Both qualitative and quantitative assessments are made part of the evaluation framework. Further, for a comparative evaluation, the real-world PNC17AFDB as well as state-of-the-art (SoA) dynamic AF Models are considered. In particular, two recent dynamic AF models, reported in [18] and [19], henceforth referred to as SoA1 and SoA2 respectively, are made part of the assessment. The reported AF model in SoA1 accounts for important AF characteristics like AF burden, varying P-wave morphology, rate of f-wave repetition, etc. The SoA2 reports the usage of a Gaussian wave-based state space to model the temporal dynamics AF ECG signals.

Visual inspection is the primary form of verification employed for evaluation of synthetic ECGs [2]. Accordingly, sample time-series plots of real-world AF from the PNC17AFDB, and synthetic AF sequences generated by the proposed AF model, SoA1 and SoA2 are shown as Fig. 6(a), Fig. 6(b), Fig. 6(c) and Fig. 6(d) respectively. Fig. 6(a) is taken as the real-world reference. Upon visual inspection of

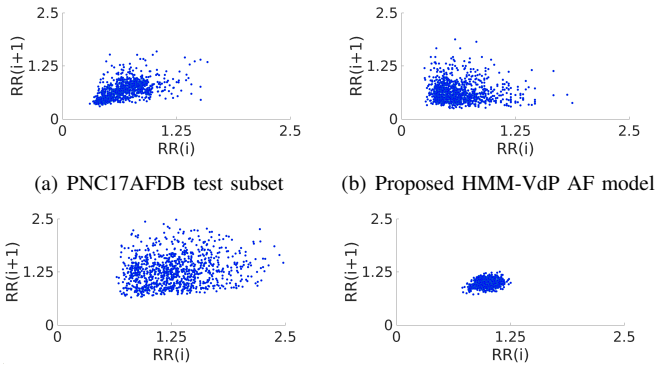

(a) PNC17AFDB test subset (b) Proposed HMM-VdP AF model

(c) SoA1 paroxysmal AF model (d) SoA2 Gaussian wave AF model

Fig. 7. Poincaré plots of real-world AF time-series and synthetic AF time-series generated by the proposed HMM-VdP AF model and existing SoAs

TABLE I
QUANTITATIVE ASSESSMENT OF THE PROPOSED AF MODEL

Method	R-peak count	P-wave count	P_{count}/R_{count}
Actual dataset (PNC17AFDB)	35333	1063	0.03
Proposed AF model	10250	5502	**0.54**
SoA1 [18]	10000	7630	0.76
SoA2 [19]	13326	16486	0.81

the figures, it can be surmised that among the three synthetic sequences, the one generated through the proposed method bears closest resemblance with the reference real-world AF signal in terms of RR interval irregularity, absence of P-wave and the presence of the fibrillatory f-waves. It can be further observed that for the sequence produced by SoA1, the RR interval variance is not as prominent as in the reference Fig. 6(a). Further, in case of SoA2 (Fig. 6(d)), the T waves are missing and the RR interval variation is even more subdued.

The next qualitative evaluation is done in terms of Poincaré plots. Poincaré plots are widely used for pattern analysis of random events [25]. In ECG domain, Poincaré plot of (RR_i, RR_{i+1}) pairs have been reported to exhibit distinct patterns for different pathological conditions, especially for arrhythmic condition like AF [20]. Accordingly, the poincaré plots of 1000 RR-interval points extracted from each of the PNC17AFDB, the proposed AF model, SoA1 and SoA2 are shown in Fig. 7(a), Fig. 7(b), Fig. 7(c) and Fig. 7(d) respectively. Similar to the case of the time-series plots, upon visual inspection of the figures, it can be surmised that among the three synthetic sequences, the Poincaré plot corresponding to the proposed AF model matches the closest with the reference PNC17AFDB Poincaré plot in terms of the cluster shape and co-ordinate location. It can be further observed that for the SoA1 Poincaré plot, the cluster spread is significantly wider and the location of the spread does not match with the reference plot either. For SoA2 Poincaré plot, the shape and spread of the data points does not match with the reference plot either. Its dense cluster indicates limited variation in the RR intervals, which is uncharacteristic of a real-world AF sequence.

The third assessment of the generated AF sequences is done

in term of a novel quantitative metric, $\rho^{R,P}$. $\rho^{P,R}$ is defined as the ratio between the count of P-waves and R-peaks that are detected by the Pan-Tomkins algorithm [24] for a given ECG sequence. By its definition, $\rho^{P,R}$ should have a value close to 1 in case of sinus rhythms and close to 0 in case of AF sequences. Hence, this metric bears particular significance for quality assessment of synthetic AF sequences. The count of R-peaks and P-waves that are detected and the corresponding values of $\rho^{P,R}$ for the PNC17AFDB, the proposed AF model, SoA1 and SoA2 are reported in Table I. The value of $\rho^{P,R}$ is close the zero for PNC17AFDB, thus corroborating with the ground-truth. Although, $\rho^{P,R}$ for the AF sequences generated by the proposed method is high (0.54), it is still a significant improvement over $\rho^{P,R}$ values corresponding to SoA1 (0.76) and SOA2 (0.81) respectively.

Hence, based on the qualitative and quantitative assessment of the proposed integrated HMM-VdP Oscillator based AF ECG model and comparative analysis with existing SoAs, it can be surmised that the proposed model is a significant improvement over the existing dynamic models for synthetic AF generation. However there exists a wide scope for improvement especially regarding the presence of P-waves.

IV. Conclusion

This paper presents a novel integrated hidden Markov model-Van Der Pol oscillator based AF model that is able to assimilate the characteristic features of AF and generate reliable synthetic AF time-series. The generated AF sequences are validated successfully through qualitative and quantitative evaluations. Further, the efficacy of the proposed AF model is substantiated through comparative assessments with existing state-of-the-art dynamic AF models. AF data generated by the presented dynamic model can be a valuable resource for education and characterization of heart diseases. Overall, it can be concluded that while the proposed model has substantially reduced the morphological-similarity gap between real-world and synthetic AF signals, there remains much room for further improvement through research and innovation.

Acknowledgement

The authors would like to acknowledge Dr. Dibyendu Roy for his valuable inputs on the AF related works during his tenure in TCS Research, Tata Consultancy Services.

References

[1] W. H. Organization, "Cardiovascular diseases (CVDs)," https://www.who.int/news-room/fact-sheets/detail/cardiovascular-diseases-(CVDs), accessed: March 5, 2025.

[2] B. Zanchi, G. Monachino, L. Fiorillo, G. Conte, A. Auricchio, A. Tzovara, and F. D. Faraci, "Synthetic ECG signals generation: A scoping review," *Comput. Biol. Med.*, vol. 184, p. 109453, 2025.

[3] A. Mukherjee, A. D. Choudhury, S. Datta, C. Puri, R. Banerjee, R. Singh, A. Ukil, S. Bandyopadhyay, A. Pal, and S. Khandelwal, "Detection of atrial fibrillation and other abnormal rhythms from ECG using a multi-layer classifier architecture," *Physiol. Meas.*, vol. 40, no. 5, p. 054006, jun 2019.

[4] U. D. of Health Human Services, "Health information privacy and accountability act (HIPAA)," https://permanent.fdlp.gov/gpo10291/fshipaa.html, accessed: March 10, 2025.

[5] S. for Economic Affairs (SECO), "New federal act on data protection (nFADP)," https://www.kmu.admin.ch/kmu/en/home/facts-and-trends/digitization/data-protection/new-federal-act-on-data-protection-nfadp.html, accessed: March 10, 2025.

[6] O. Sayadi, M. B. Shamsollahi, and G. D. Clifford, "Synthetic ECG generation and Bayesian filtering using a Gaussian wave-based dynamical model," *Physiol. Meas.*, vol. 31, no. 10, p. 1309, 2010.

[7] M. A. Quiroz-Juárez, O. Jiménez-Ramírez, J. Aragón, J. L. Del Río-Correa, and R. Vázquez-Medina, "Periodically kicked network of rlc oscillators to produce ECG signals," *Comput. Biol. Med.*, vol. 104, pp. 87–96, 2019.

[8] G. Monachino, B. Zanchi, L. Fiorillo, G. Conte, A. Auricchio, A. Tzovara, and F. D. Faraci, "Deep generative models: The winning key for large and easily accessible ECG datasets?" *Comput. Biol. Med.*, vol. 167, p. 107655, 2023.

[9] F. N. Hatamian, N. Ravikumar, S. Vesal, F. P. Kemeth, M. Struck, and A. Maier, "The effect of data augmentation on classification of atrial fibrillation in short single-lead ECG signals using deep neural networks," in *ICASSP 2020-2020 IEEE International Conference on Acoustics, Speech and Signal Processing (ICASSP)*. IEEE, 2020, pp. 1264–1268.

[10] E. Ryzhii and M. Ryzhii, "A heterogeneous coupled oscillator model for simulation of ECG signals," *Comput. Methods Programs Biomed.*, vol. 117, no. 1, pp. 40–49, 2014.

[11] P. E. McSharry, G. D. Clifford, L. Tarassenko, and L. A. Smith, "A dynamical model for generating synthetic electrocardiogram signals," *IEEE Trans. Biomed. Eng.*, vol. 50, no. 3, pp. 289–294, 2003.

[12] G. C. Cardarilli, L. Di Nunzio, R. Fazzolari, M. Re, and F. Silvestri, "Improvement of the cardiac oscillator based model for the simulation of bundle branch blocks," *Appl. Sci.*, vol. 9, no. 18, p. 3653, 2019.

[13] R. FitzHugh, "Impulses and physiological states in theoretical models of nerve membrane," *Biophys. J.*, vol. 1, no. 6, pp. 445–466, 1961.

[14] J. Nagumo, S. Arimoto, and S. Yoshizawa, "An active pulse transmission line simulating nerve axon," *Proceedings of the IRE*, vol. 50, no. 10, pp. 2061–2070, 1962.

[15] H. Kamel, P. M. Okin, M. S. Elkind, and C. Iadecola, "Atrial fibrillation and mechanisms of stroke: time for a new model," *Stroke*, vol. 47, no. 3, pp. 895–900, 2016.

[16] F. Censi, I. Corazza, E. Reggiani, G. Calcagnini, E. Mattei, M. Triventi, and G. Boriani, "P-wave variability and atrial fibrillation," *Sci. Rep.*, vol. 6, no. 1, p. 26799, 2016.

[17] J. Heijman, H. Sutanto, H. J. Crijns, S. Nattel, and N. A. Trayanova, "Computational models of atrial fibrillation: Achievements, challenges, and perspectives for improving clinical care," *Cardiovasc. Res.*, vol. 117, no. 7, pp. 1682–1699, 2021.

[18] A. Petrenas, V. Marozas, A. Sološenko, R. Kubilius, J. Skibarkiene, J. Oster, and L. Sörnmo, "Electrocardiogram modeling during paroxysmal atrial fibrillation: application to the detection of brief episodes," *Physiol. Meas.*, vol. 38, no. 11, p. 2058, nov 2017.

[19] M. A. Quiroz-Juárez, J. A. Rosales-Juárez, O. Jiménez-Ramírez, R. Vázquez-Medina, and J. L. Aragón, "ECG patient simulator based on mathematical models," *Sensors*, vol. 22, no. 15, p. 5714, 2022.

[20] S. Sarkar, D. Ritscher, and R. Mehra, "A detector for a chronic implantable atrial tachyarrhythmia monitor," *IEEE Trans. Biomed. Eng.*, vol. 55, no. 3, pp. 1219–1224, 2008.

[21] Q. Wang, W. Wang, Y. Wang, J. Ren, and B. Zhang, "Multi-stage network attack detection algorithm based on Gaussian mixture hidden markov model and transfer learning," *IEEE Trans. Autom. Sci. Eng.*, vol. 22, pp. 3470–3484, 2025.

[22] L. R. Rabiner, "A tutorial on hidden markov models and selected applications in speech recognition," *Proceedings of the IEEE*, vol. 77, no. 2, pp. 257–286, 1989.

[23] G. D. Clifford, C. Liu, B. Moody, H. L. Li-wei, I. Silva, Q. Li, A. Johnson, and R. G. Mark, "Af classification from a short single lead ECG recording: The physionet/computing in cardiology challenge 2017," in *2017 Computing in Cardiology (CinC)*. IEEE, 2017, pp. 1–4.

[24] J. Pan and W. J. Tompkins, "A real-time qrs detection algorithm," *IEEE Trans. Biomed. Eng.*, vol. BME-32, no. 3, pp. 230–236, 1985.

[25] K. S. Franz, S. Rezaei, and T. Chau, "Elucidating interpersonal cardiac synchrony during a naturalistic social interaction using dyadic poincaré plot analysis," *IEEE Access*, 2024.